Development of a Hybrid Nanocarrier Recognized Tumor Vasculature and Penetrated BBB for Glioblastoma Multi-Targeting Therapy

Rangrang Fan[1,†], Di Chuan[1,†], Huan Hou[1], Haifeng Chen[1],

Bo Han[2], Xiaoning Zhang[3], Liangxue Zhou[1], Aiping Tong[1,*],

Jianguo Xu[1,*], Gang Guo[1,*]

[1] State Key Laboratory of Biotherapy and Cancer Center, and Department of Neurosurgery, West China Hospital, Sichuan University, and Collaborative Innovation Center for Biotherapy, Chengdu, 610041, PR China

[2] School of Pharmacy, Key Laboratory of Xinjiang Phytomedicine Resource and Utilization, Ministry of Education, School of Medicine, Shihezi University, Xinjiang Shihezi 832003, PR China

[3]Department of Pharmacology and Pharmaceutical Sciences, School of Medicine, Tsinghua University, Beijing 100084, PR China

[*]Corresponding author.Tel.: +86 28 85164063; Fax.:+86 2885164060.
E-mail addresses:guogang@scu.edu.cn (G. Guo),xujg_2001@126.com(J. G. Xu), aipingtong@scu.edu.cn (A. P. Tong)

[†]These authors contributed equally to this work.

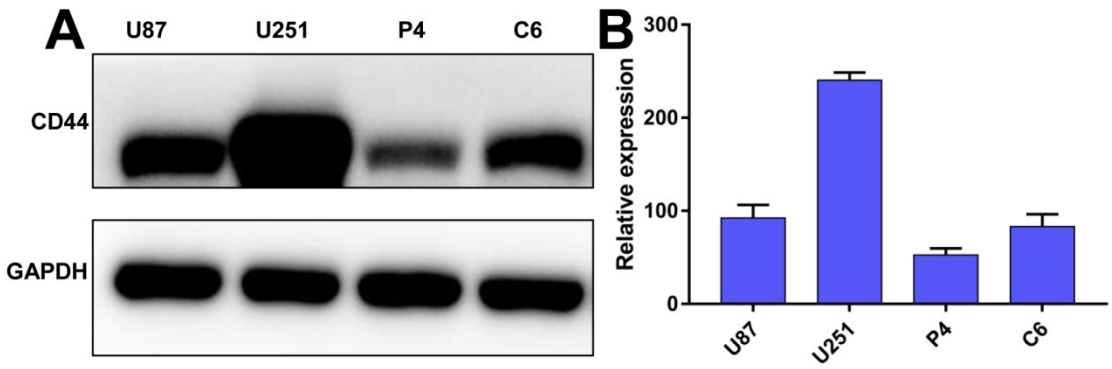

Fig. S1 Western blots were employed to test the protein levels of CD44 (A), and CD44 expression was quantified by the densitometry analysis using Image J (B).

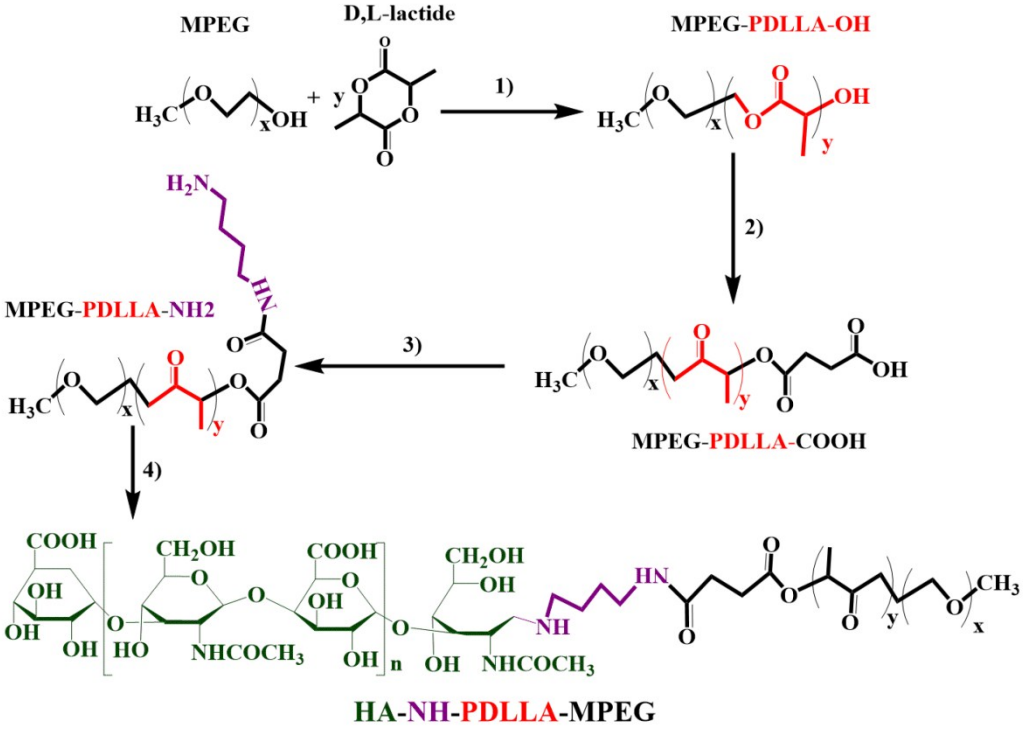

Fig.S2 Synthesis of HA-modified MPEG-PDLLA, 1) 0.3% Sn(Oct)2, 140 °C. 2) 2 eq. succine anhydride, 1 eq. TEA and 1 eq. DMAP in 1,4-dioxane; 3) 10 eq. 1,4-diaminobutane, 1 eq. EDCI, 1 eq. HOBT and 5 eq. TEA in anhydrous DMF; 4) 1.5 eq. HA and 20 eq. sodium cyanoborohydride in acetate buffer (pH=5.6).

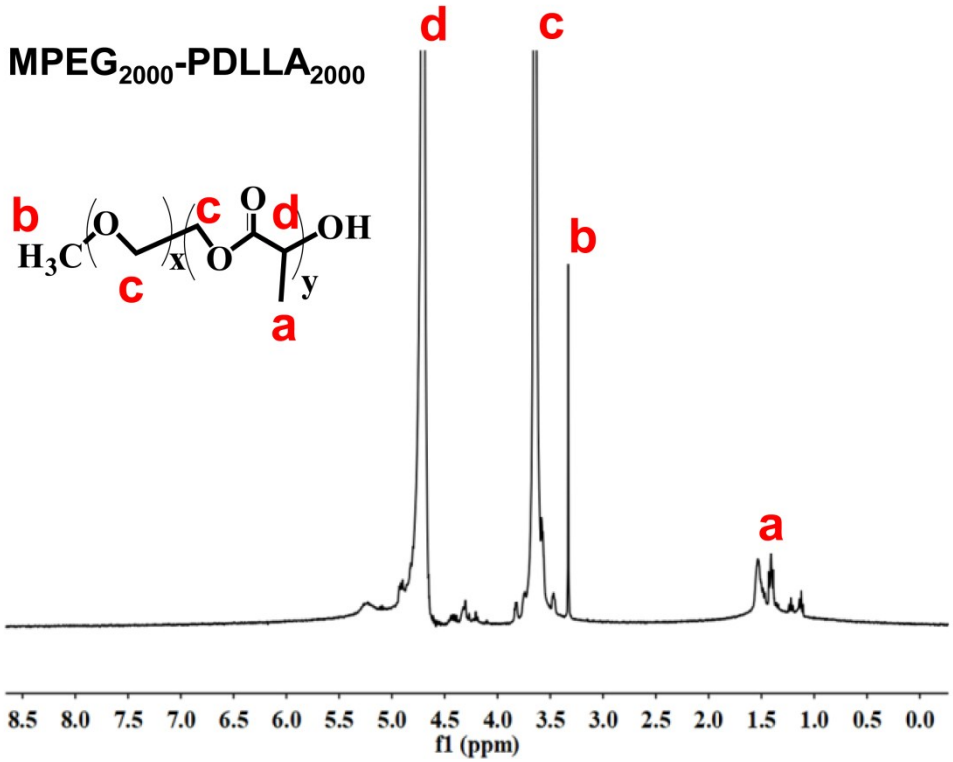

Fig.S3 ^{1}H-NMR spectra of $MPEG_{2000}$-$PDLLA_{2000}$.

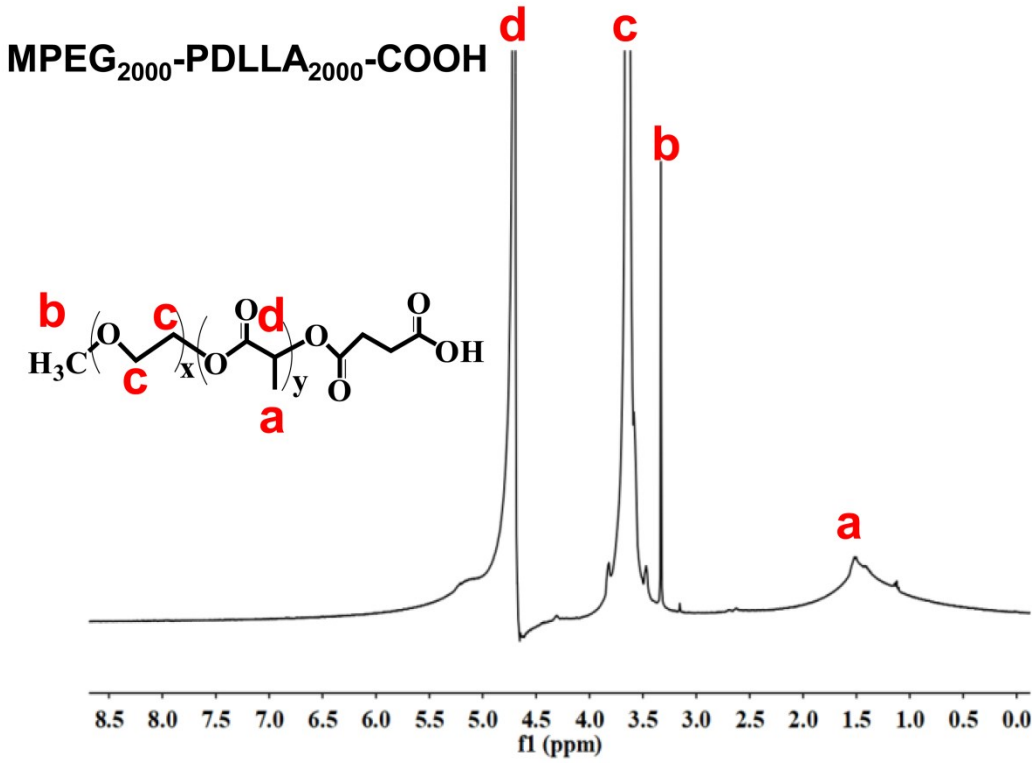

Fig.S4 ^{1}H-NMR spectra of $MPEG_{2000}$-$PDLLA_{2000}$-COOH.

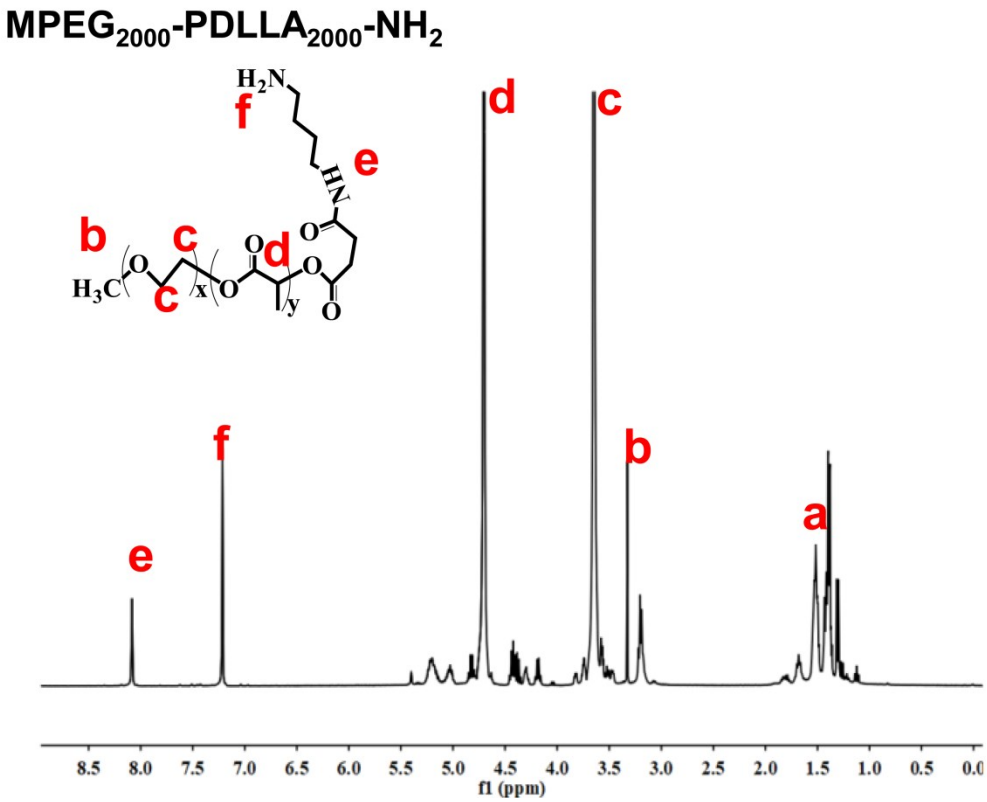

Fig.S5 ^{1}H-NMR spectra of $MPEG_{2000}$-$PDLLA_{2000}$-NH_2.

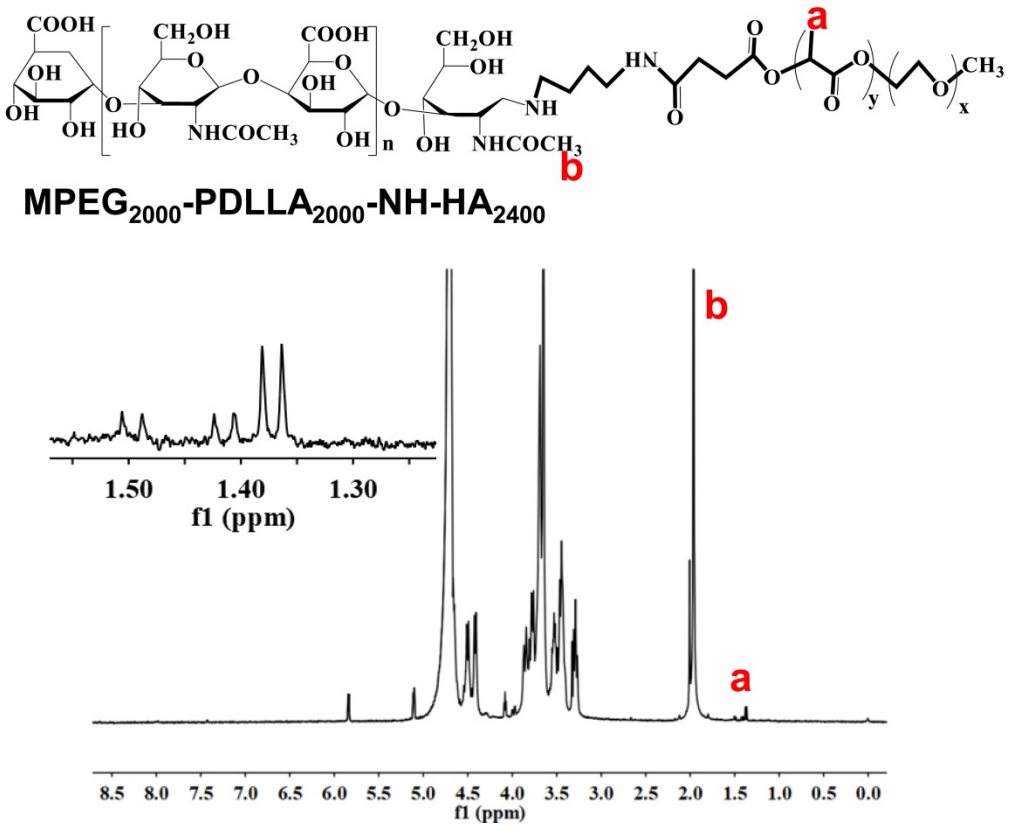

Fig.S6 ^{1}H-NMR spectra of $MPEG_{2000}$-$PDLLA_{2000}$-NH-HA_{2400}.

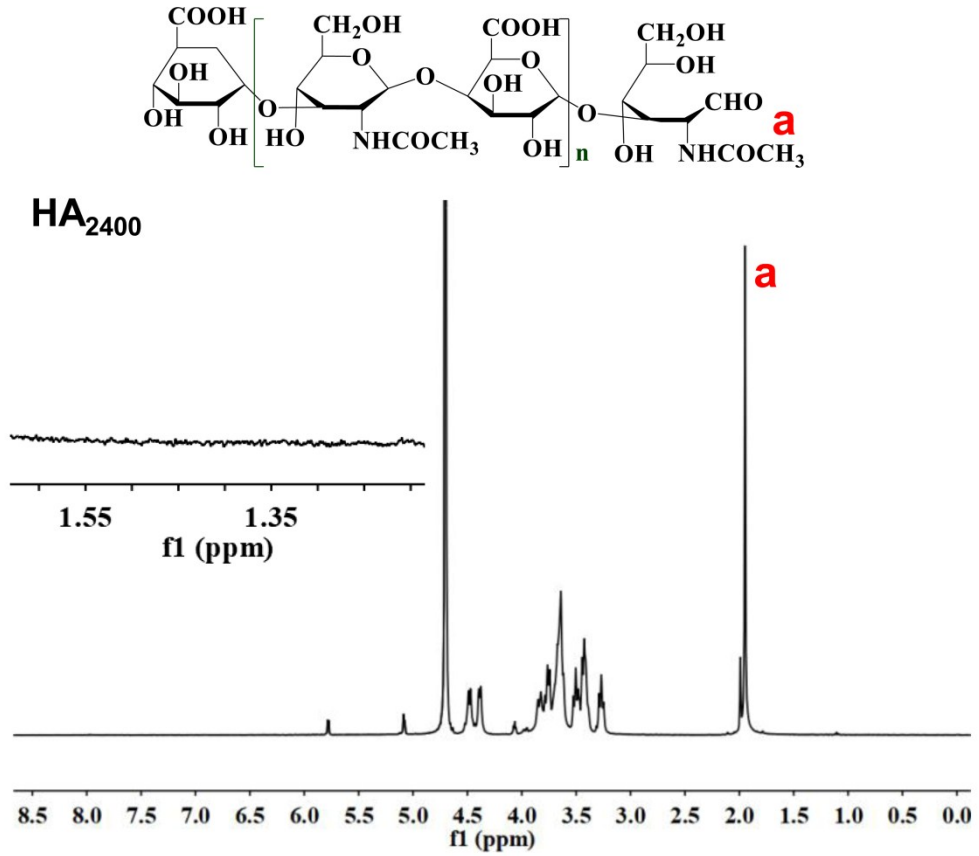

Fig.S7 ^{1}H-NMR spectra of HA_{2400}.

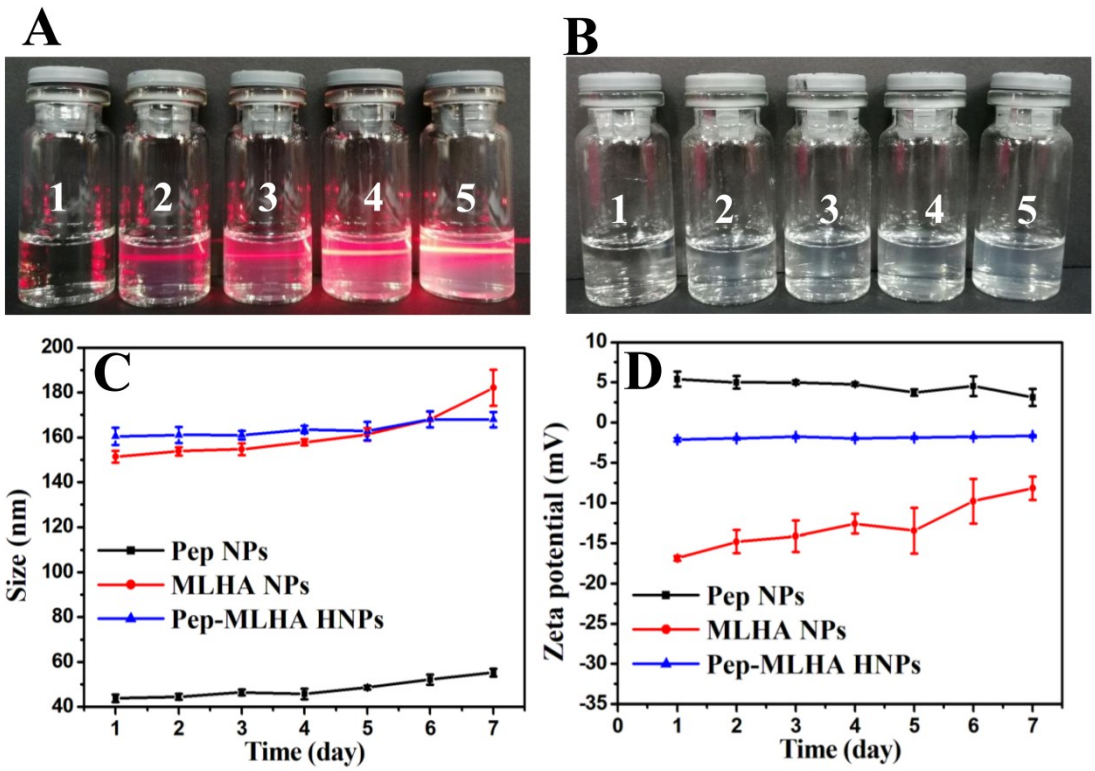

Fig.S8 Preparation of DTX/Pep-MLHA HNPs. (A) Prepared nanoparticles. (B) Prepared nanoparticles were placed at room temperature for one week. The stability of prepared nanoparticles evaluated by (C) size and (D) zeta potential change within one week in PBS (pH 7.4) at 37 ^{o}C. (1) Deionized water, (2) MLHA NPs, (3) DTX/ML NPs, (4) DTX/MLHA NPs, (5) DTX/Pep-MLHA HNPs. (C) Size and (D) zeta potential change within one week in PBS (pH =7.4) at 37 ^{o}C.

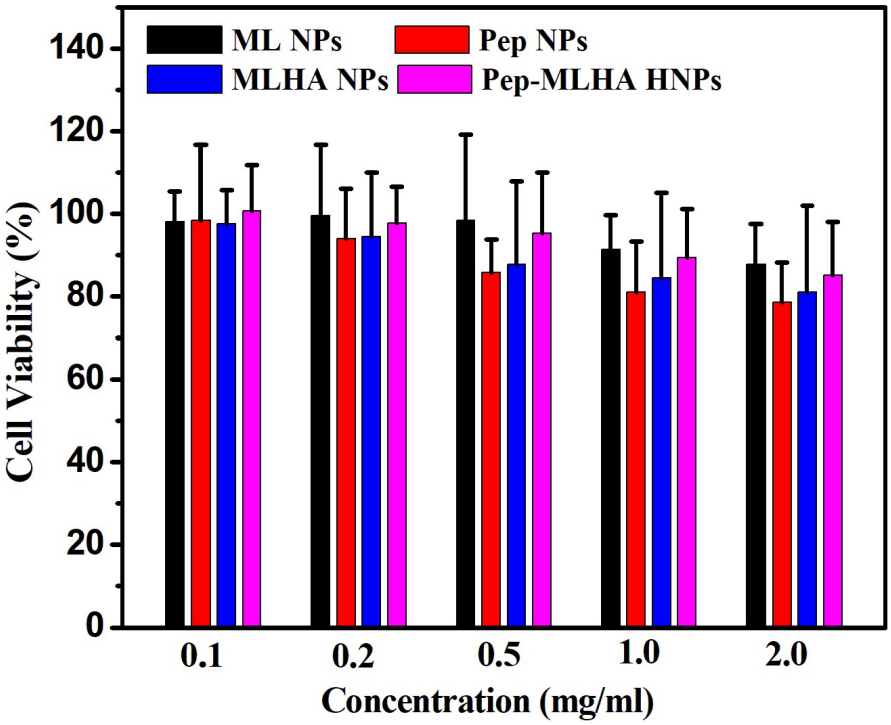

Fig.S9 *In vitro* cytotoxicity assay of blank ML NPs, Pep NPs, MLHA NPs and Pep-MLHA HNPs.

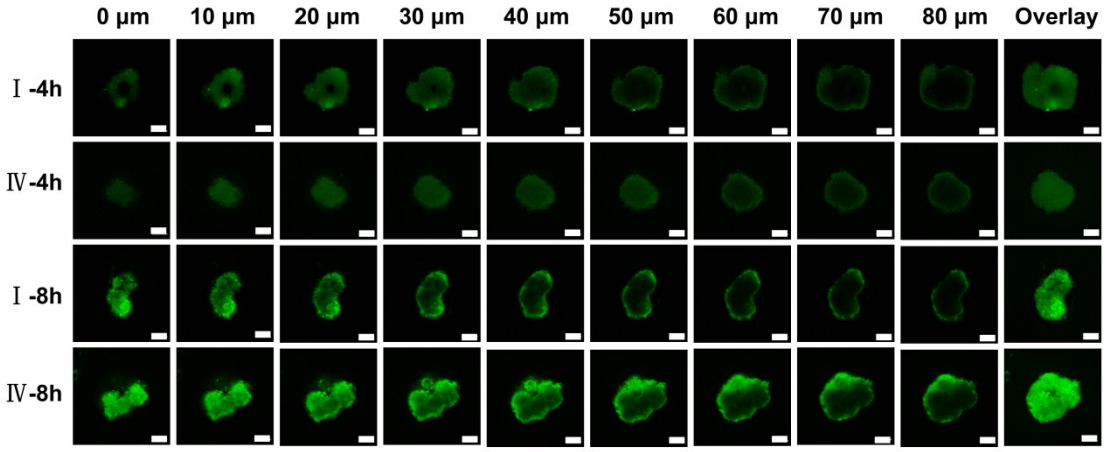

Fig.S10 C6 tumor spheroids uptake of coum-6/ML NPs (Ⅰ), coum-6/Pep-MLHA HNPs (Ⅳ), the scale bar represents 200 μm.

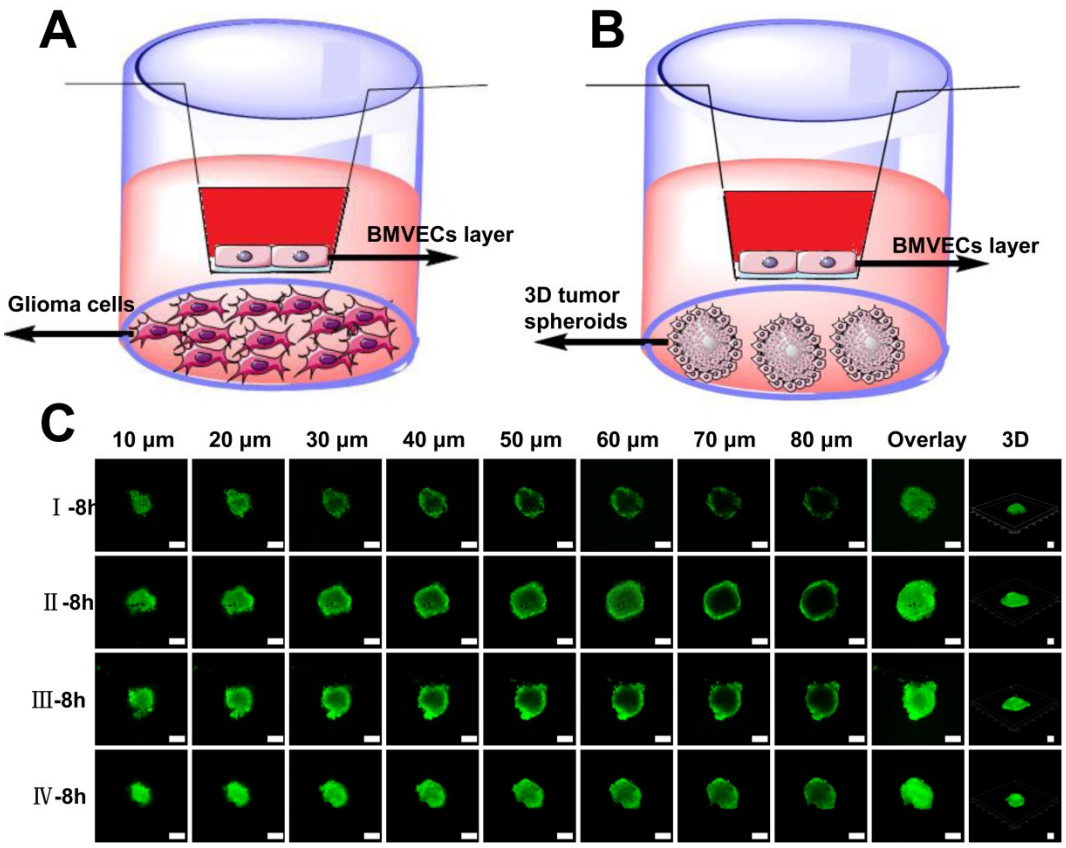

Fig.S11 The BBB model study. Schematic illustration of the *in vitro* BBB model using a transwell system to evaluate intracellular distribution of coum-6 fluorescence in glioma cells (A) and 3D tumor spheroids (B) after transporting across the BBB. (C) Distribution of Coum-6 fluorescence in C6 tumor spheroids after transporting across the BBB, the scale bar represents 200 μm. (Ⅰ) Coum-6/ML NPs, (Ⅱ) Coum-6/Pep NPs, (Ⅲ) Coum-6/MLHA NPs and (Ⅳ) Coum-6/Pep-MLHA HNPs.

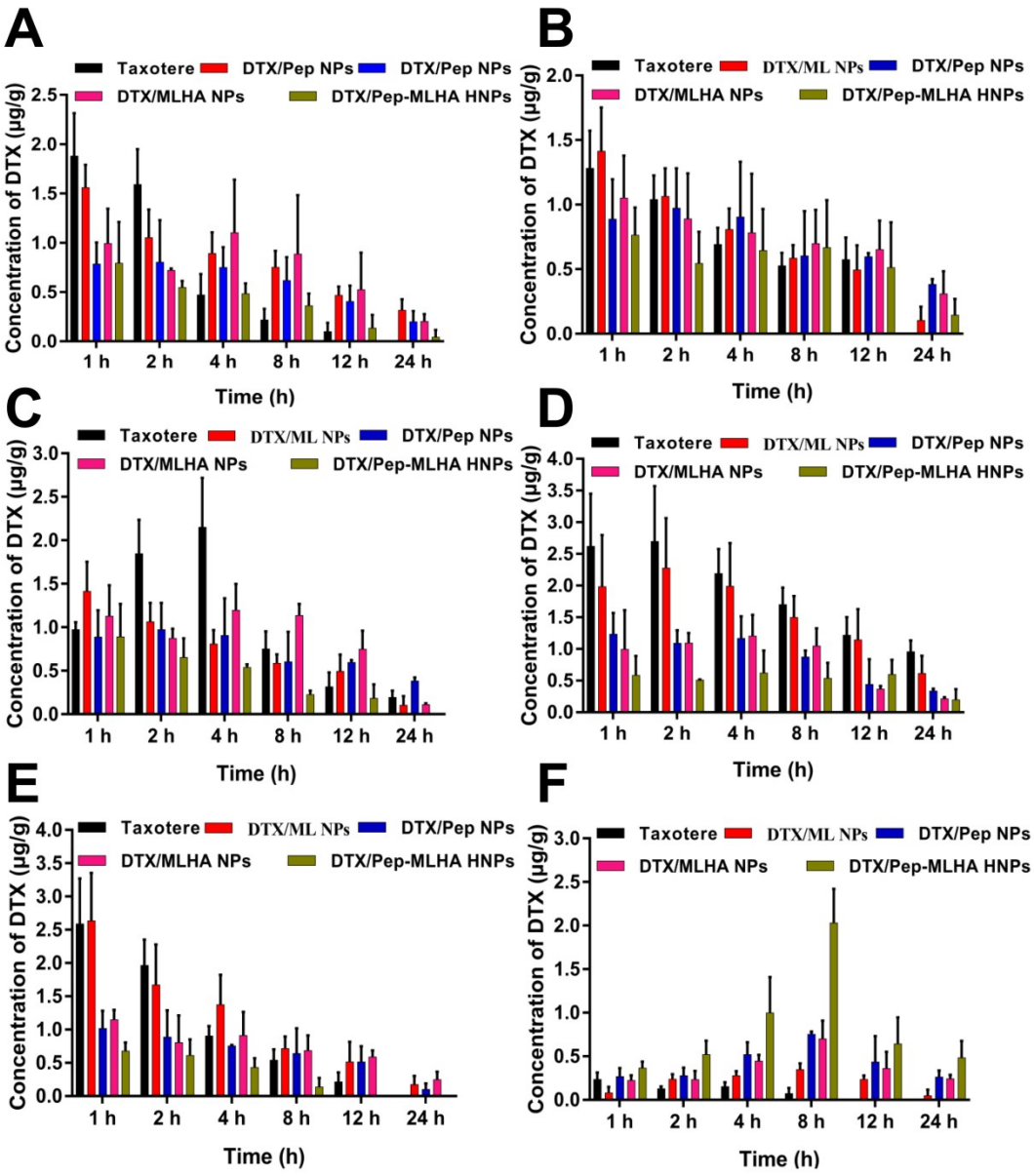

Fig.S12 Biodistribution profile of different DTXformulations in (A) Heart (B) Liver (C) Spleen (D Lungs (E) Kidney and (F) brain at a dose of 10 mg/kg of DTX in intracranial glioma bearing Sprague–Dawley rats. The data represent the mean ± SD (n=3).

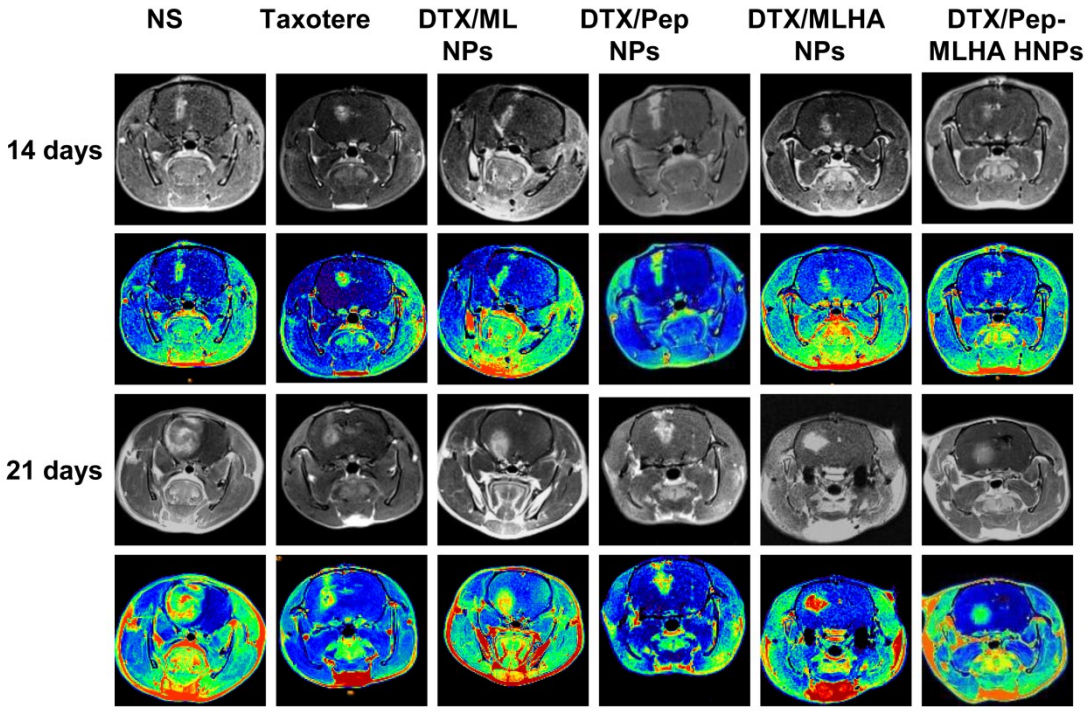

Fig.S13 Visualization of C6 glioma tumor growth inhibition using MR imaging at the time point 14 and 21 days after the first injection.

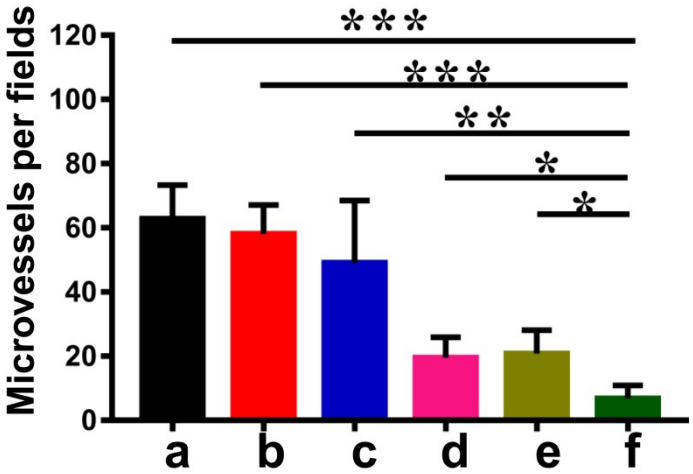

Fig.S14 The microvessel density (MVD) in each group. (a) NS, (b) Taxtere®, (c) DTX/ML NPs, (d) DTX/Pep NPs, (e) DTX/MLHA NPs, (f) DTX/Pep-MLHA HNPs. $^{*}p < 0.05$, $^{**}p < 0.01$, $^{***}p < 0.001$.